ACCSCIENCE PUBLISHING

International Journal of Bioprinting

CASE STUDY

Neuromodulation with a 3D-printed, patient-specific hand orthotic in stroke: A proof-of-concept fMRI case series on clinical application

Zikai Hua[1]*, Zhipeng Li[1], and Ying Zhang[2,3]*

[1]School of Mechatronic Engineering and Automation, Shanghai University, Shanghai, China

[2]Department of Rehabilitation, Shanghai Xuhui Central Hospital, Shanghai, China

[3]Longhua Hospital Affiliated to Shanghai University of Traditional Chinese Medicine, Shanghai, China

(This article belongs to the *Special Issue: 3D Printing in Clinical Application*)

Abstract

Three-dimensional (3D) printing holds great promise for creating patient-specific rehabilitative devices. While previous studies have demonstrated that behavioral interventions can induce cortical reorganization in stroke, direct evidence that a device alone—specifically, a patient-specific 3D-printed orthotic—can modulate brain function remains lacking. This proof-of-concept case series bridges this gap by integrating a complete digital workflow—from upper limb 3D scanning to stereolithography (SLA) fabrication of a custom hand orthotic—with longitudinal multimodal functional magnetic resonance imaging (fMRI) to assess cortical reorganization in chronic stroke. Four patients participated, with two index cases wearing the 3D-printed orthosis daily for four months alongside conventional rehabilitation, while two reference patients underwent conventional therapy only. Pre- and post-intervention neuroimaging revealed consistent, orthosis-associated neural changes: enhanced activity in the primary somatosensory cortex and greater functional integration within sensorimotor networks. Structural adaptations in motor regions were also observed in both index cases. Quantitatively, the index cases exhibited functional changes in nine brain regions and structural changes in six regions, substantially exceeding the minimal changes observed in the reference cases. This work provides the first direct evidence that a 3D-printed, patient-specific orthotic can drive targeted neuroplasticity independent of intensive behavioral coaching, validating its role not merely as a passive assistive device but as an active neuromodulatory tool. It establishes a translational framework for using objective neuroimaging biomarkers to guide the development and personalization of 3D-printed interventions in neurorehabilitation.

Keywords: 3D printing; Additive manufacturing; Stroke rehabilitation; Neuromodulation; Functional MRI; Proof-of-concept study

***Corresponding authors:**
Zikai Hua
(eddie_hua@shu.edu.cn)
Ying Zhang
(ZhangYing032317@163.com)

Citation: Hua Z, Li Z, Zhang Y. Neuromodulation with a 3D-printed, patient-specific hand orthotic in stroke: A proof-of-concept fMRI case series on clinical application. *Int J Bioprint*. 2026:12(2):026050035. doi: 10.36922/IJB026050035

Received: January 28, 2026

Revised: March 15, 2026

Accepted: March 23, 2026

Published online: April 24, 2026

1. Introduction

Three-dimensional (3D) printing, or additive manufacturing, is revolutionizing personalized medicine by enabling the rapid fabrication of anatomical structures and medical devices tailored to the individual patient.[1–3] In neurorehabilitation, this technology holds particular promise for creating patient-specific orthotics that perfectly conform to a patient's unique morphology, potentially improving comfort, adherence, and biomechanical efficacy. Upper limb motor impairment, affecting up to 80% of stroke survivors, represents a prime target for such personalized interventions.[4–8]

A growing body of work has begun to explore the application and effect of 3D printing in this domain.[3,9–15] Cui *et al.*[16] reviewed a large body of literature and found that 3D-printed, patient-specific orthoses can prevent and correct upper limb deformities, maintain limbs in functional positions, provide traction to prevent joint contractures, partially compensate for the function of disabled muscles, and aid in the treatment of upper limb motor dysfunction. Ang *et al.*[14] demonstrated, through a combination of design and experimentation, that 3D-printed wrist orthoses can effectively restore at least 70% of the range of motion in healthy individuals. Zheng *et al.*[15] compared the rehabilitation effects of low-temperature thermoplastic splints and 3D-printed orthoses, finding that 3D-printed orthoses were superior in reducing spasticity and swelling in stroke patients, improving wrist joint motor function, and enhancing the passive extension range of the wrist joint compared to low-temperature thermoplastic splints. However, the existing evidence remains largely confined to peripheral assessments of motor performance, symptom improvement, comfort, and biomechanical function.

Parallel to this line of device-focused research, a separate and well-established body of work has demonstrated that the central nervous system retains significant plasticity and can be remodeled by rehabilitation. Seminal work by Levy *et al.*,[17] using constraint-induced movement therapy (CIMT), provided functional MRI evidence that intensive behavioral protocols can induce cortical reorganization in chronic stroke patients. This discovery fundamentally alters the understanding of stroke recovery, demonstrating that the adult brain can undergo significant reorganization through targeted behavioral therapy.

However, these prior demonstrations of neuroplasticity have emerged almost exclusively from therapist-intensive behavioral interventions. Whether a device alone—specifically, a patient-specific 3D-printed orthotic engineered for optimal biomechanical interaction—can serve as a sufficient driver of neuroplasticity remains entirely unexplored. This distinction is critical: if a device can actively engage neural circuits without requiring constant therapist guidance, it would have profound implications for scalability, accessibility, and the mechanistic understanding of how physical interfaces with the body influence brain reorganization. Therefore, the innovation of the present study lies in showing that a precisely engineered, personalized orthotic can be an active agent in that process, independent of intensive behavioral coaching. This represents a fundamental shift from intervention-as-behavior to intervention-as-device.

Resting-state functional magnetic resonance imaging (fMRI) provides a powerful, non-invasive method to quantify such brain plasticity. By measuring intrinsic neural activity through blood-oxygen-level-dependent (BOLD) signals,[18] it can reveal reorganization within functional networks.[18,19] To capture a comprehensive picture, we employed a multimodal fMRI approach, analyzing the amplitude of low-frequency fluctuations (ALFF), its fractional component (fALFF), and regional homogeneity (ReHo). This combination allows for the concurrent assessment of local metabolic intensity and functional coherence, offering complementary insights into both functional and structural aspects of neuroplastic change.

Here, we present a proof-of-concept case series that bridges this critical gap between advanced manufacturing and systems neuroscience. We aimed to characterize the cortical reorganization induced by a 3D-printed, patient-specific hand orthotic in chronic stroke patients. By integrating a complete digital design-and-fabrication workflow with longitudinal, multimodal fMRI, this study seeks to provide the first direct evidence that a 3D-printed medical device can, independent of intensive behavioral coaching, elicit specific and measurable neurobiological effects, thereby establishing a foundational framework for biologically informed design and personalized application in neurorehabilitation.

2. Case presentation

2.1. Descriptions

All cases were patients of the Department of Rehabilitation, Shanghai Xuhui Central Hospital. Consent was obtained from all patients prior to their participation for using their personal data for research purposes. This study was conducted in strict adherence to the Declaration of Helsinki, and this study was approved by the Ethics Committee of Shanghai Xuhui Central Hospital. All data were processed in an irreversible and anonymous manner, and the risks posed to participants in this study are minimal.

2.1.1. Patients receiving combined 3D-printed orthotic and conventional therapy (index cases)

Case 1 was a 66-year-old female suffering from intracerebral hemorrhage, with lesion located at the right basal ganglia region. The patient underwent a 4-month intervention with a patient-specific hand orthosis, combined with conventional upper limb rehabilitation therapy.

Case 2 was a 72-year-old male suffering from cerebral infarction, with lesion located at the left temporal and parieto-occipital lobes. The patient underwent a 4-month intervention with a patient-specific hand orthosis, combined with conventional upper limb rehabilitation therapy.

2.1.2. Patients receiving conventional therapy alone (reference cases)

Case 3 was an 87-year-old male suffering from intracerebral hemorrhage, with lesion located at the right basal ganglia and frontotemporal lobes. During the same period, the patient received only conventional upper limb rehabilitation therapy, serving as a reference for observing the natural recovery process of brain changes.

Case 4 was a 69-year-old male suffering from cerebral infarction, with lesion located at the right basal ganglia region. During the same period, the patient received only conventional upper limb rehabilitation therapy, serving as a reference for observing the natural recovery process of brain changes.

2.2. Device fabrication and mechanical validation

The orthosis shown in Figure 1 is patient-specific for each individual participant. The process began with scanning the patient's upper limb using the Go!Scan optical scanner (Creaform Inc., Canada). The resulting 3D model of the upper limb was imported into Geomagic Studio software for repair, followed by modeling in Unigraphics NX software. Subsequently, the model was sliced in UNIZ Desktop software and 3D-printed using the UNIZ Slash Pro stereolithography printer. This printer offers a precision of up to 20 μm, with adjustable layer thickness resolution options of 10, 25, 50, 100, 150, 200, and 300 μm. It achieves a maximum printing speed of 200 mm/h, making it a device that combines both high precision and speed. The material used was medical-grade photosensitive resin, specifically the Zabs (UNIZ) model, which is safe, non-toxic, and exhibits minimal allergenicity and irritation. It also possesses excellent mechanical properties and a high surface finish. Printed at a speed of 200 mm/h, the orthosis underwent secondary curing in a SimpNeed curing chamber to complete the fabrication. Before each use, the surface of the orthosis was wiped with 70% ethanol for disinfection and sterilization.

Material testing. Tensile tests were performed on standardized specimens (n = 5 per condition) fabricated using the same printer and resin as the orthotics (Figure 2A). The testing was conducted in adherence to the Chinese national standards (GB/T 1040.1-2018, GB/T 1040.2-2006) using a AGS-X-300kN electronic universal testing machine produced by Shimadzu Instrume (Suzhou) Co., Ltd.

Finite element analysis. A 3D model of the orthotic was imported into the Abaqus software (Dassault SIMULIA, Providence, Rhode Island, USA). A static torque of 14.81 N·m was applied to the palmar region to simulate wrist

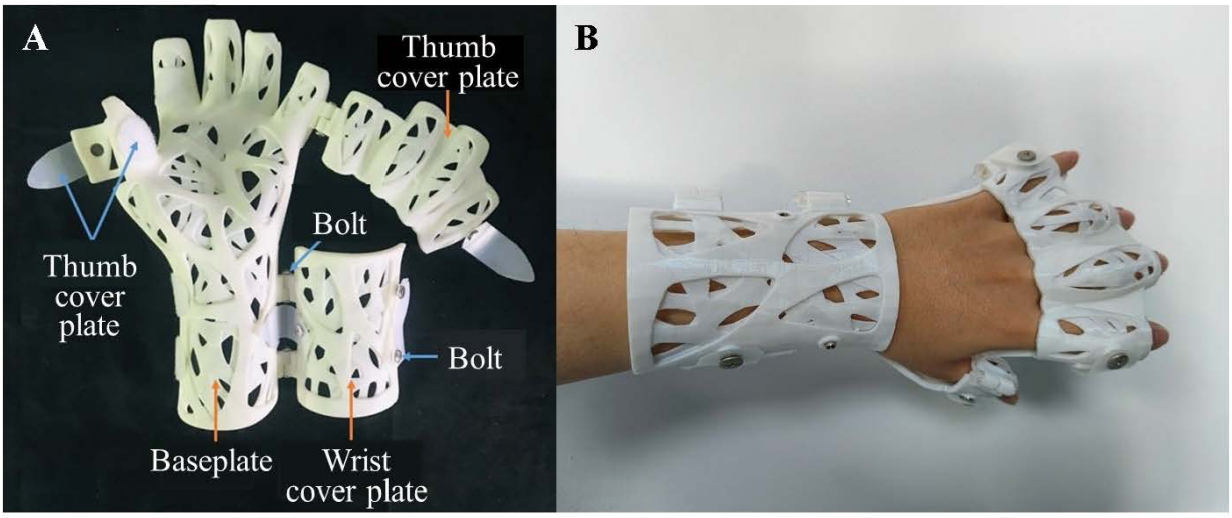

Figure 1. The orthotic developed independently by our team (A) and its appearance after use (B)

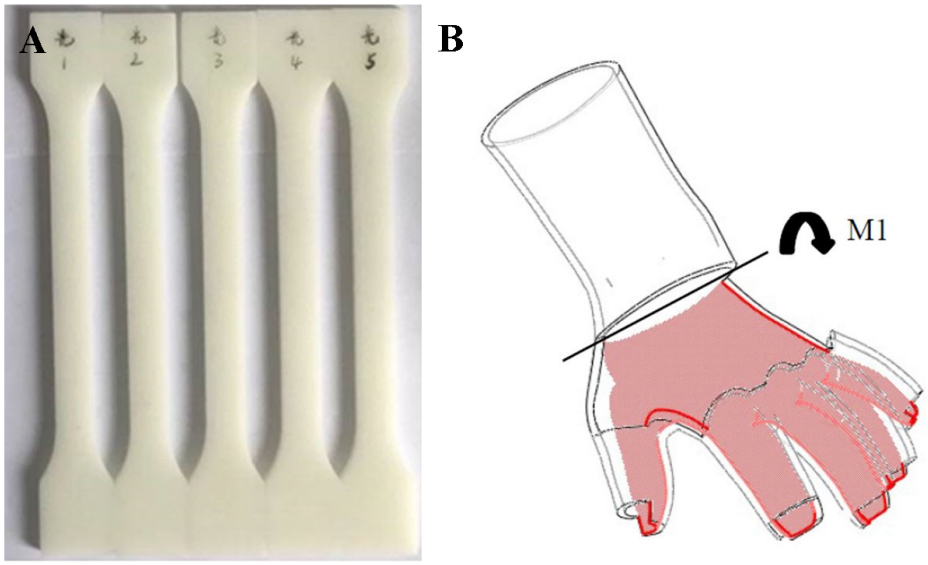

Figure 2. Standard specimen used in tensile test (A) and schematic diagram of force application (B)

flexion in patients,[20] while constraints were imposed on the wrist contact surface to replicate real-world wearing conditions (Figure 2B). The von Mises stress distribution was calculated and compared with the material yield strength obtained from tensile tests.

2.3. Treatment procedure

In a 4-month intervention, the patients in reference cases received conventional rehabilitation treatments, including physical therapy and occupational therapy, for 2 to 3 h daily, 5 days a week. In addition to the conventional rehabilitation treatment, the patients in index cases wore the orthosis for 4–8 h daily, 5 days a week. Each subject underwent fMRI data collection both at baseline (month 0) and after the rehabilitation treatment (after 4 months). The detailed process is shown in Figure 3.

2.4. fMRI imaging acquisition

MRI data were acquired using a 1.5 Tesla Siemens scanner (Siemens Healthineers, German). For each participant, we obtained:

(i) Structural images: T1-weighted MPRAGE sequence (TR/TE = 2200/2.86 ms, flip angle 8°, voxel size 1 × 1 × 1 mm^3, 176 sagittal slices).
(ii) Resting-state functional images: Gradient-echo EPI sequence (TR/TE = 2300/30 ms, flip angle 90°, voxel size 3.5 × 3.5 × 3.5 mm^3, 36 axial slices, 120 volumes, 4 min 44 s).

During functional scans, patients were instructed to keep their eyes closed, remain awake, and lie still. Total acquisition time was approximately 11 min per session. Detailed sequence parameters are available upon request.

2.5. fMRI imaging processing

All MRI data were processed using DPABI (V4.3, Institute of Psychology, Chinese Academy of Sciences, China). Functional images were preprocessed using DPARSF, including: removal of the first 10 volumes, slice timing correction, head motion correction, co-registration to structural images, spatial normalization to MNI space (3 × 3 × 3 mm^3), and smoothing (4-mm FWHM Gaussian kernel). Linear detrending was applied. For ALFF and fALFF analyses, the unfiltered low-frequency signal was used. For ReHo analysis, band-pass filtering (0.01–0.08 Hz) was applied to remove physiological noise. Structural images were processed using DPABISurf within a Docker environment for cortical surface reconstruction. Quality control excluded datasets with excessive head motion (>2.5 mm translation or >2.5° rotation). Given the within-subject design, paired-sample analyses were performed to compare pre- and post-intervention metrics. Multiple comparison correction was applied at the cluster level (FWE-corrected $p < 0.05$). Baseline comparisons confirmed no significant differences between index and reference cases prior to intervention.

3. Results

3.1. Mechanical validation of the 3D-printed orthotic

Material testing confirmed that the photosensitive resin exhibited a tensile strength of 34.28 MPa and an elastic modulus of 678.82 GPa. Finite element analysis showed

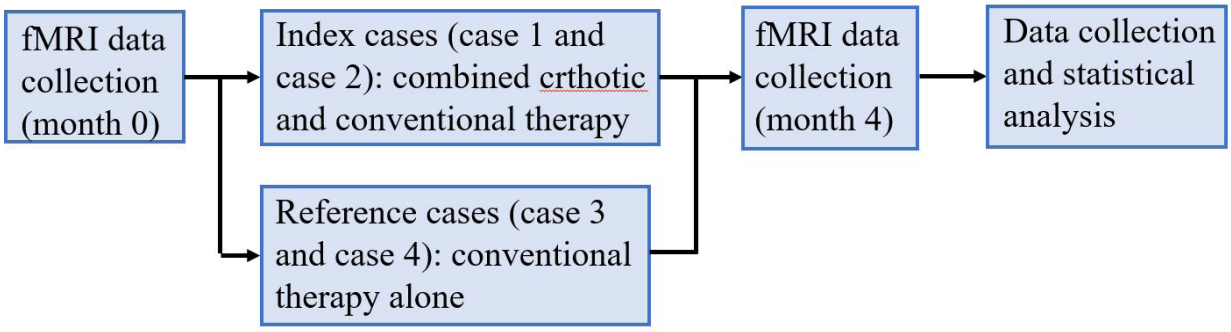

Figure 3. Treatment and experimental procedure

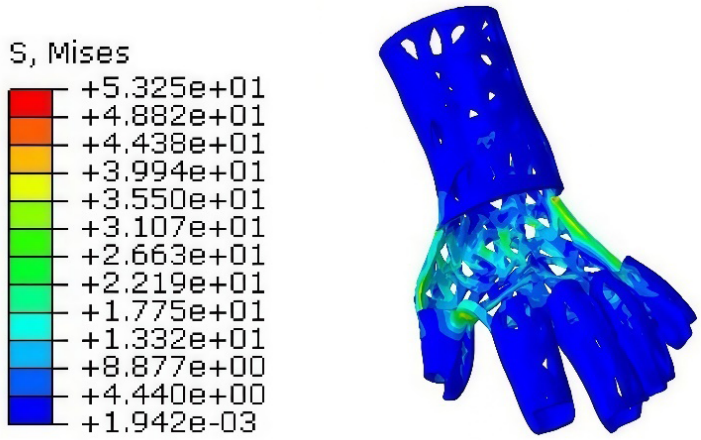

Figure 4. Finite element analysis results

that under simulated gripping load, the maximum von Mises stress in the orthotic was 53.25 MPa (Figure 4), which is lower than the material's yield strength (68.9 MPa). Given that the load parameters applied in this study significantly exceed the realistic load conditions, the device can withstand daily use without mechanical failure. This also ensures the accuracy of subsequent fMRI experiments.

3.2. Brain function results

For the brain images presented in Figures 5–7, warm-colored regions (red) indicate brain areas where the activity intensity post-treatment is higher than pre-treatment; cool-colored regions (blue) indicate areas where the activity intensity pre-treatment is higher than post-treatment.

Regarding the somatosensory and temporal regions, Increased neural activity was consistently observed in the primary somatosensory cortex (right postcentral gyrus), as reflected by elevated fALFF values in Figure 5. Temporal lobe regions, including the bilateral inferior temporal gyrus, right middle temporal gyrus, and left superior temporal gyrus, also exhibited enhanced activity across multiple metrics (ALFF/fALFF). These findings suggest augmented sensory processing and integration following orthotic use.

Regarding parietal and occipital regions, the right superior occipital gyrus, left angular gyrus, and right supramarginal gyrus showed increased fALFF or ReHo, indicating enhanced functional coherence within visuospatial and somatosensory association networks.

Regarding frontal region, increased ReHo in the left inferior frontal gyrus suggests improved local functional synchronization (Figure 6), potentially related to motor planning or attention.

In contrast, the reference cases demonstrated minimal changes, with only three regions showing alterations (left supramarginal gyrus, right inferior parietal lobule, and left middle occipital gyrus), as shown in Figure 7.

3.3. Brain structure results

Structural changes were observed predominantly in the index cases, as shown in Figure 8. Key findings include increased cortical measures in motor-related regions, namely the left precentral gyrus (primary motor cortex)

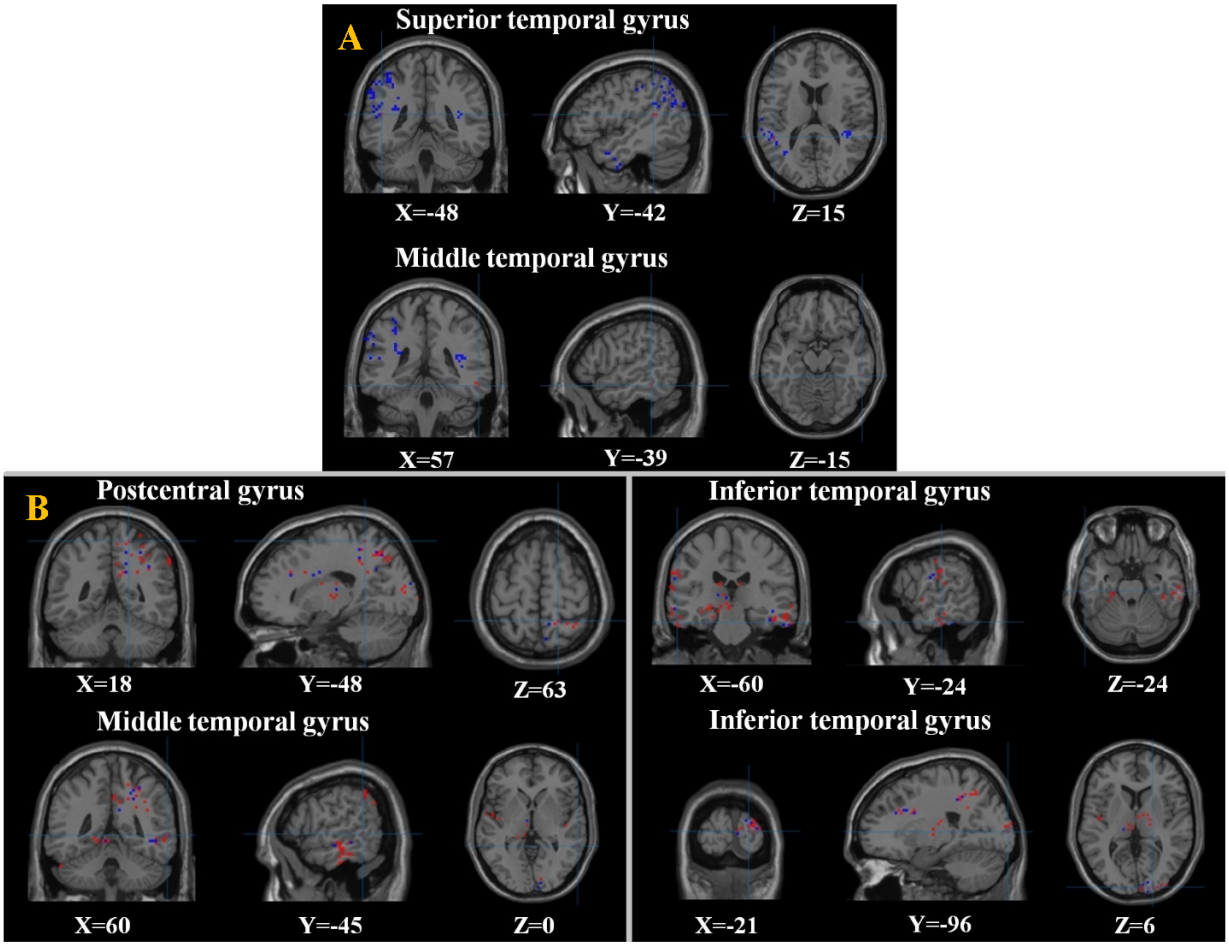

Figure 5. Brain region functional imaging results of the index cases. (A) Differences in ALFF brain regions before and after treatment of the index cases. (B) Differences in fALFF brain regions before and after treatment of the index cases.

Abbreviations: ALFF: Amplitude of low-frequency fluctuations; fALFF: Fractional amplitude of low-frequency fluctuation.

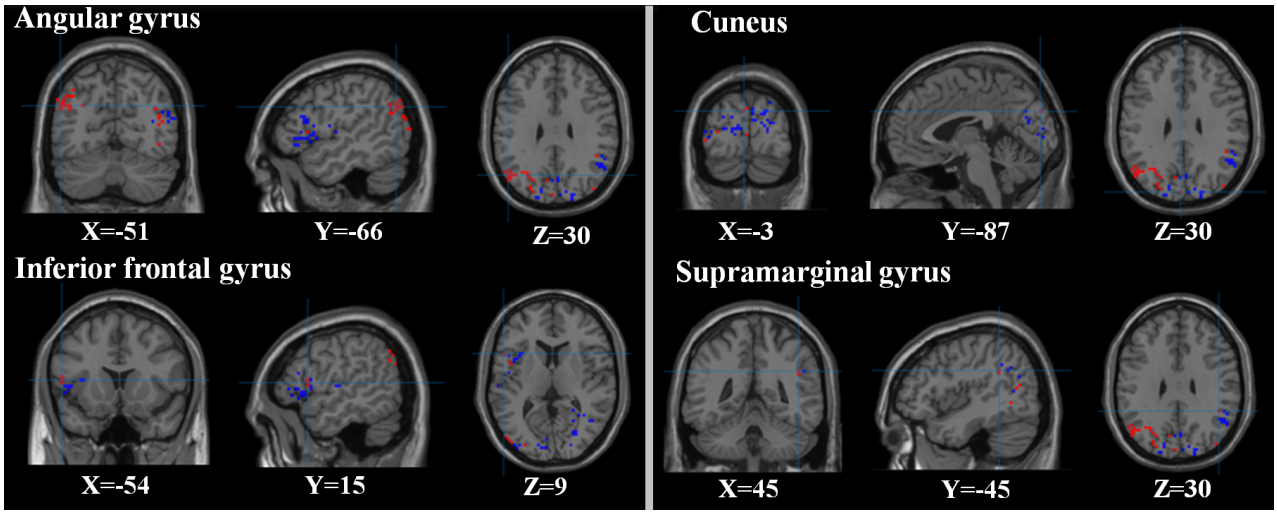

Figure 6. Differences in regional homogeneity (ReHo) brain regions before and after treatment of the index cases

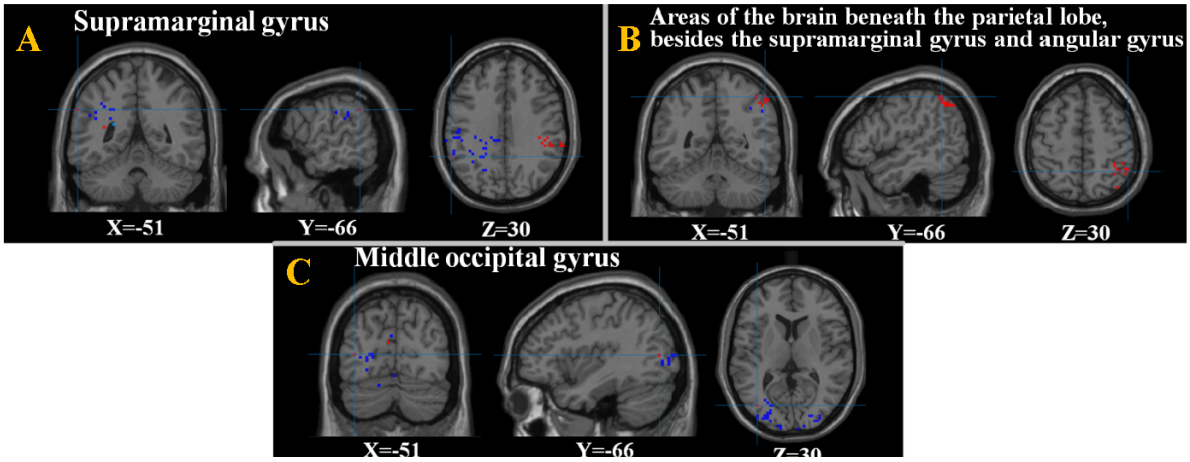

Figure 7. Brain region functional imaging results of the reference cases. (A) Differences in ALFF brain regions before and after treatment of the reference cases. (B) Differences in fALFF brain regions before and after treatment of the reference cases. (C) Differences in ReHo brain regions before and after treatment of the reference cases.
Abbreviations: ALFF: Amplitude of low-frequency fluctuations; fALFF: Fractional amplitude of low-frequency fluctuation; ReHo: Regional homogeneity.

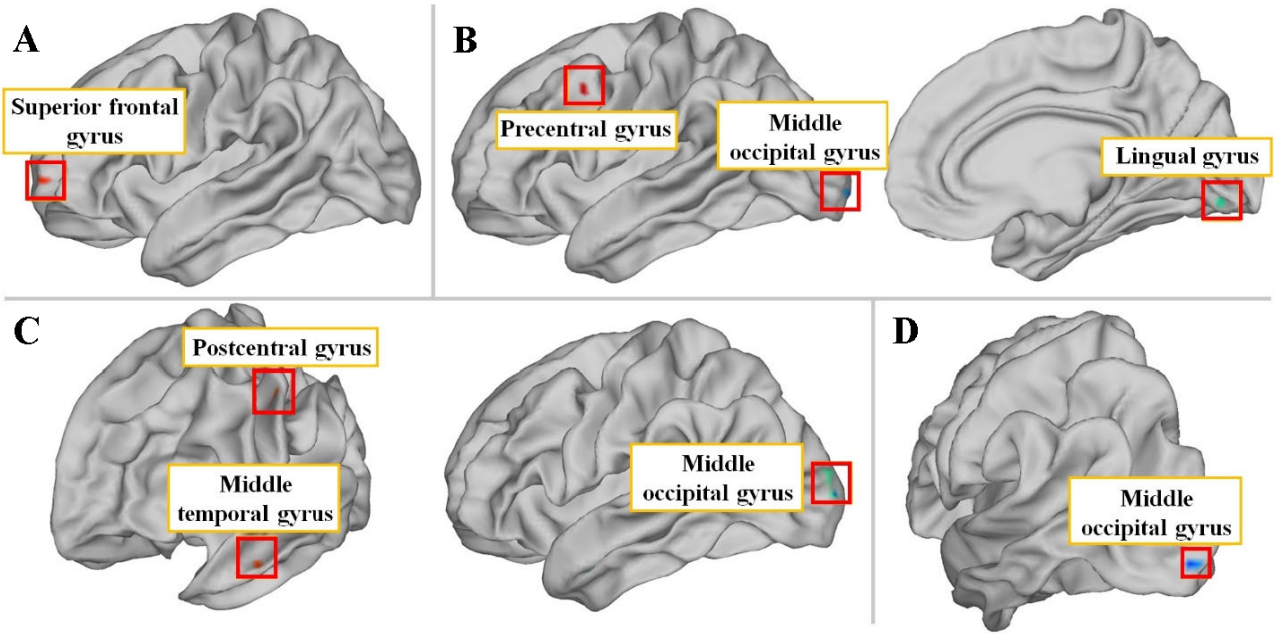

Figure 8. Brain region structural imaging results. (A) ALFF cortical surface projection maps before and after treatment in the index cases. (B) fALFF cortical surface projection maps before and after treatment in the index cases. (C) ReHo cortical surface projection maps before and after treatment in the index cases. (D) fALFF cortical surface projection maps before and after treatment in the reference cases. The purpose of the red squares is to mark the areas where structural changes have occurred.
Abbreviations: ALFF: Amplitude of low-frequency fluctuations; fALFF: Fractional amplitude of low-frequency fluctuation; ReHo: Regional homogeneity.

and left superior frontal gyrus (adjacent to supplementary motor area). Additionally, structural enhancement was noted in the left postcentral gyrus (somatosensory cortex) and left middle temporal gyrus, which are the regions showing functional changes.

In the reference cases, only the left middle occipital gyrus exhibited structural alteration, with a negative peak intensity indicating decreased measures post-intervention.

4. Discussion

After compilation, functional imaging alterations were observed in 11 distinct brain regions, as detailed in Table 1. Based on the results of brain function imaging, we found that in the index cases, the neural activity in the right

Table 1. The brain regions showing differences in functional imaging between the two groups before and after treatment

	Brain region with the highest peak	Peak	Voxel	BA	Laterality	MNI coordinate (mm)		
						X	Y	Z
Index cases								
ALFF	Superior temporal gyrus	+	440	41	Left	−48	−42	15
	Middle temporal gyrus	+	94	21	Right	57	−39	−15
fALFF	Postcentral gyrus	+	232	2	Right	18	−48	63
	Middle temporal gyrus	+	99	21	Right	60	−45	0
	Inferior temporal gyrus	+	81	20	Left	−60	−24	−24
	Superior occipital gyrus	+	69	18	Right	21	−96	6
ReHo	Angular gyrus	+	193	39	Left	−51	−66	30
	Inferior frontal gyrus	+	134	44	Left	−54	15	9
	Cuneus	+	95	18	Left	−3	−87	30
	Supramarginal gyrus	+	91	40	Right	45	−45	30
Reference cases								
ALFF	Supramarginal gyrus	+	412	40	Left	−60	−48	33
fALFF	Areas of the brain beneath the parietal lobe, besides the supramarginal gyrus and angular gyrus	+	73	40	Right	51	−51	54
ReHo	Middle occipital gyrus	+	315	19	Left	−39	−75	9

Abbreviations: ALFF: Amplitude of low-frequency fluctuations; BA: Brodmann area; fALFF: Fractional amplitude of low-frequency fluctuation; ReHo: Regional homogeneity.

hemisphere postcentral gyrus significantly increased after treatment. The postcentral gyrus, located in the parietal lobe of the brain and posterior to the central sulcus, is the primary somatosensory cortex (S1), adjacent to the primary motor cortex. S1 is a key area for processing somatosensory information. Meier *et al.*[21] conducted an fMRI experiment where participants wore a motion-controlled hand exoskeleton and observed significant activation in the S1 region. This indicates that the S1 region can directly receive and process sensory information from the hand, such as touch, pain, and itch. In our experiment, the 3D-printed, patient-specific orthosis kept the patient's palm in a resting position while providing continuous contact on the palm's inner side, which, with long-term use, enhanced the patient's tactile sensation. Consequently, the activation of the S1 region was observed in the brain function imaging. Many scholars believe that activation of brain regions related to specific tasks can aid in the functional recovery of the brain in stroke patients.[17,22,23] Currently, there are two views on brain function recovery in stroke patients. Some scholars believe that damaged neurons can be repaired,[24,25] thereby restoring brain function. However, this view has been challenged in recent years. It has been argued that the repair capacity of neurons is very limited, and recovery occurs primarily through the reorganization of new neurons, which replace the function of the damaged neurons.[26,27] Constraint-induced therapy, such as wearing a 3D-printed orthosis, is believed to accelerate the process of new neuron reorganization, thus facilitating recovery.[17]

Furthermore, this activation phenomenon also reflects the compensatory strategy in brain repair,[26] wherein more extensive and diffuse activation of both motor and non-motor regions near the damaged motor area occurs to compensate for lost motor function, a phenomenon known as the recruitment effect. During stroke recovery, in order to avoid spasms during movement, widespread recruitment effects occur across various brain regions.[28] After treatment, five brain regions in the index cases showed increased ALFF or fALFF values, displaying brighter blood oxygen level-dependent (BOLD) signals in larger areas, compared to only two regions in the reference cases. This suggests that new neurons were activated to form new pathways to compensate for lost connections, promoting further functional recovery of the brain.

In contrast, the reference cases showed fewer brain regions with changes after treatment, and these changes were less associated with movement and tactile sensations. Most of the brain region changes observed in the reference cases were also seen in the index cases. The total number of changed brain regions in the index cases was three times

Table 2. The brain regions showing differences in structural imaging between the two groups before and after treatment

	Brain region with the highest peak	Peak	Laterality	Neural networks	Cortex area (mm^2)	Peak index	MNI coordinate (mm)		
							X	Y	Z
Index cases									
ALFF	Superior frontal gyrus	+	Left	Frontoparietal network	24.80	4109	−20	62	2
	Precentral gyrus	+	Left	Default network	22.88	8655	−39	10	39
fALFF	Middle occipital gyrus	-	Left	Visual network	25	9667	−21	−100	−4
	Lingual gyrus	-	Right	Visual network	22.19	2494	12	−83	−9
	Postcentral gyrus	+	Left	Somatomotor network	21.86	4513	−49	−19	39
ReHo	Middle temporal gyrus	+	Left	Default network	22.64	7048	−53	−7	−25
	Middle occipital gyrus	-	Left	Visual network	45.24	6909	−22	−98	10
Reference cases									
fALFF	Middle occipital gyrus	-	Left	Visual network	25	9667	7	−107	−25

Abbreviations: ALFF: Amplitude of low-frequency fluctuations; fALFF: Fractional amplitude of low-frequency fluctuation; ReHo: Regional homogeneity.

greater than that in the reference cases, indicating that wearing a 3D-printed orthosis on top of conventional upper limb therapy further enhances the patient's rehabilitation outcome.

Structural imaging alterations were observed in six distinct brain regions, as detailed in Table 2. From the results of brain structural imaging, the changes in each brain region show certain differences compared with functional imaging. The most significant difference is the simultaneous observation of enhanced neural activities in the left precentral gyrus and superior frontal gyrus. The precentral gyrus is located in front of the central sulcus of the frontal lobe of the brain and is the main component of the primary motor cortex (M1), which is directly responsible for functions such as the execution, coordination, and feedback of upper-limb movements in the human body. After administering training for hand motor functions using virtual reality devices, Schuster-Amft *et al.*[29] found a significant activation phenomenon in the M1 area of the patients' brains. The superior frontal gyrus is located in the upper part of the frontal lobe of the brain, adjacent to the supplementary motor area (SMA) and the premotor area (PMA). It is an area between motor and cognitive functions, mainly engaged in motor planning and decision-making, providing conditions for fine hand movements. After four months of wearing the orthosis, the patients' palms were fixed in the extended position, which avoided palm spasm, contracture, and the increment of muscle tone, thereby enhancing the hand motor functions. In addition, most fine hand movements involve the fingers. 3D-printed orthosis can spread out the five fingers of the patients and provide continuous support, further enhancing the fine motor ability of fingers. Based on the theory of neural plasticity, after a stroke, the levels of many growth factors increase within a few weeks. Through mechanisms such as neurogenesis, synaptogenesis, angiogenesis, reduced apoptosis, stem cell proliferation, and immune regulation, spontaneous neural reorganization is promoted, enabling compensatory adaptations of the brain to injury.[22,30] Therefore, through continuous physical support for the hands, neural activities in the precentral gyrus and superior frontal gyrus of the patients are jointly enhanced.

In the reference cases, the only brain region with structural changes after treatment was the middle occipital gyrus. Since structural changes require long-term and strong stimulation, the areas with structural improvement are usually fewer than those with functional improvement. The total number of brain regions with changes in two patients in the index cases was six times that in the reference cases. Due to the lack of the restricted movement and orthopedic functions of patient-specific orthoses in the reference cases, the structural improvement was generally poor.

These findings establish a critical translational link between an advanced manufacturing technique and a measurable neurobiological outcome. By demonstrating that a 3D-printed, patient-specific orthotic can induce functional and structural reorganization within sensorimotor networks, we provide the first direct evidence that additive manufacturing can be leveraged not only for anatomical customization but also for targeted neuromodulation.

Two specific attributes of the 3D-printed device, which distinguish it from conventional static splints, likely contributed to these neural effects. First, the anatomical precision achieved through 3D scanning ensures a near-perfect fit, providing continuous, congruent sensory input to the palmar surface. This sustained tactile stimulation—impossible with ill-fitting conventional splints—directly accounts for the observed S1 activation. Second, the design freedom afforded by stereolithography-based fabrication a lightweight, hollowed structure that minimizes patient burden while maintaining mechanical integrity. This reduced biomechanical interference allows patients to engage in more natural movement attempts, potentially facilitating the recruitment of motor planning regions such as the superior frontal gyrus.

The implications for the field of 3D printing in medicine are significant. Our work moves the application of this technology in rehabilitation from a "form-fitting" paradigm to a "function-eliciting" paradigm. For engineers and clinicians, this suggests that future design optimization can be biologically informed. Parameters such as contact surface texture (to modulate tactile stimulation) or precise joint angulation (to influence proprioceptive input and motor planning) can now be iterated with the explicit goal of maximizing desirable neural responses, as quantified by fMRI biomarkers like ALFF or ReHo.

As a proof-of-concept case series, this study has inherent limitations, including a small sample size and the absence of concurrent standardized clinical outcome measures, which precludes definitive correlation between neural changes and functional gains. However, within the context of exploratory translational research, these limitations are offset by the unique value of providing an in-depth, mechanistic validation of a 3D-printed medical device. The detailed neurophenotyping serves as an essential hypothesis-generating resource for the interdisciplinary community. In the future, we will expand the sample size and conduct more intensive experiments using iteratively improved orthoses to further verify their impact on the brain.

5. Conclusion

This proof-of-concept case series provides foundational neuroimaging evidence that a 3D-printed, patient-specific hand orthotic can function as an active neuromodulatory device in stroke rehabilitation. By integrating longitudinal, multimodal resting-state fMRI (employing ALFF, fALFF, and ReHo analyses) in index patients who received the orthotic intervention alongside reference cases, we directly visualized its central effects. The intervention was associated with consistent and targeted cortical reorganization. Quantitatively, the index cases exhibited functional changes in nine brain regions and structural changes in six regions, substantially exceeding the minimal changes observed in the reference cases. Key findings include significantly enhanced neural activity within the primary somatosensory cortex and more extensive functional integration across sensorimotor networks compared to conventional therapy. Notably, structural adaptations in motor-planning regions were also observed. These changes, which were markedly more widespread than those seen with standard care, align with the proposed dual mechanism of augmented tactile feedback and stabilized functional posture facilitated by the custom-fit device.

Collectively, this work establishes a crucial translational link between additive manufacturing and measurable neuroplasticity. Critically, it provides the first evidence that a precisely engineered, personalized device can drive targeted neuroplasticity independent of intensive behavioral coaching—a fundamental shift from intervention-as-behavior to intervention-as-device. This moves the application of 3D-printed orthotics beyond anatomical customization into the realm of targeted neuromodulation. The identified fMRI signatures offer objective biomarkers for future research, paving the way for a new paradigm of biomarker-guided, personalized neurorehabilitation.

Acknowledgments

None.

Funding

This work was self-funded by the authors.

Conflict of interest

The authors declared no potential conflicts of interest with respect to the research, authorship, and/or publication of this article.

Author contributions

Conceptualization: Zikai Hua, Ying Zhang
Formal analysis: Zikai Hua, Zhipeng Li
Investigation: Zikai Hua
Methodology: Zikai Hua, Ying Zhang
Writing–original draft: Zhipeng Li
Writing–review & editing: Zikai Hua, Zhipeng Li

Ethics approval and consent to participate

This study was approved by the Ethics Committee of Shanghai Xuhui Central Hospital (approval ID: KESHE (2022) No.056). Written consent of all patients has been obtained.

Consent for publication

Written consent of all patients has been obtained for publishing their data and images.

Availability of data

The data that support the findings of this study are available from the corresponding author, upon reasonable request.

References

1. Ledoux ED, Barth EJ. Design, modeling, and preliminary evaluation of a 3D-printed wrist–hand grasping orthosis for stroke survivors. *Wearable Technol.* 2024;5:e12.

   doi: 10.1017/wtc.2024.18

2. Bose D, Gupta S, Chanda A. Scalable direct manufacturing of a functional multipurpose wrist-hand orthosis using 3D printing. *Ann 3D Print Med.* 2025;17:100186.

   doi: 10.1016/j.stlm.2025.100186

3. Demeco A, Foresti R, Frizziero A, *et al*. The Upper Limb Orthosis in the Rehabilitation of Stroke Patients: The Role of 3D Printing. *Bioengineering.* 2023;10(11):1256.

   doi: 10.3390/bioengineering10111256

4. Gorelick PB. The global burden of stroke: persistent and disabling. *Lancet Neurol.* 2019;18(5):417-418.

   doi: 10.1016/S1474-4422(19)30030-4

5. The GBD 2016 Lifetime Risk of Stroke Collaborators. Global, regional, and country-specific lifetime risks of stroke, 1990 and 2016. *New Engl. J. Med.* 2018;379(25):2429-2437.

   doi: 10.1056/NEJMoa180449

6. He Q, Wang W, Zhang Y, *et al*. Global, regional, and national burden of stroke, 1990–2021: A systematic analysis for global burden of disease 2021. *Stroke*. 2024;55(12):2815-2824.

   doi: 10.1161/STROKEAHA.124.048033

7. Cantillo-Negrete J, Carino-Escobar RI, Carrillo-Mora P, *et al*. Brain-Computer Interface Coupled to a Robotic Hand Orthosis for Stroke Patients' Neurorehabilitation: A Crossover Feasibility Study. *Front Hum Neurosci.* 2021;15:656975.

   doi: 10.3389/fnhum.2021.656975

8. Vaughn S, Cournan M. World Health Organization Rehabilitation 2030: Call to Action Update. *Rehabil Nurs J.* 2024;49(5):143-146.

   doi: 10.1097/RNJ.0000000000000473

9. Toth L, Schiffer A, Nyitrai M, *et al*. Developing an anti-spastic orthosis for daily home-use of stroke patients using smart memory alloys and 3D printing technologies. *Mater Des.* 2020;195:109029.

   doi: 10.1016/j.matdes.2020.109029

10. Oud TAM, Lazzari E, Gijsbers HJH, *et al*. Effectiveness of 3D-printed orthoses for traumatic and chronic hand conditions: A scoping review. *PloS ONE.* 2021;16(11):e0260271.

    doi: 10.1371/journal.pone.0260271

11. Yang YS, Tseng CH, Fang WC, Han IW, Huang SC. Effectiveness of a New 3D-Printed Dynamic Hand–Wrist Splint on Hand Motor Function and Spasticity in Chronic Stroke Patients. *J Clin Med*. 2021;10(19):4549.

    doi: 10.3390/jcm10194549

12. Wang K, Shi Y, He W, *et al*. The research on 3D printing fingerboard and the initial application on cerebral stroke patient's hand spasm. *BioMedical Eng.* 2018;17(1):92.

    doi: 10.1186/s12938-018-0522-4

13. Schlaug G, Cassarly C, Feld JA, *et al*. Safety and efficacy of transcranial direct current stimulation in addition to constraint-induced movement therapy for post-stroke motor recovery (TRANSPORT2): a phase 2, multicentre, randomised, sham-controlled triple-blind trial. *Lancet Neurol.* 2025;24(5):400-412.

    doi: 10.1016/S1474-4422(25)00044-4

14. Ang BWK, Yeow CH. Design and Characterization of a 3D Printed Soft Robotic Wrist Sleeve with 2 DoF for Stroke Rehabilitation. In: Proceedings of the 2019 2nd IEEE International Conference on Soft Robotics (RoboSoft); April 14-18, Seoul, South Korea. IEEE; 2019:577-582.

    doi: 10.1109/ROBOSOFT.2019.8722771

15. Zheng Y, Liu G, Yu L, Wang Y, Fang Y, Shen Y, *et al*. Effects of a 3D-printed orthosis compared to a low-temperature thermoplastic plate orthosis on wrist flexor spasticity in chronic hemiparetic stroke patients: a randomized controlled trial. *Clin Rehabil.* 2019;34(2):194-204.

    doi: 10.1177/0269215519885174

16. Cui Y, Cheng S, Chen X, Xu G, Ma N, Li H, *et al*. Advances in the clinical application of orthotic devices for stroke and spinal cord injury since 2013. *Front Neurol.* 2023;14.

    doi: 10.3389/fneur.2023.1108320

17. Levy CE, Nichols DS, Schmalbrock PM, *et al*. Functional MRI evidence of cortical reorganization in upper-limb stroke hemiplegia treated with constraint-induced movement therapy. *Am J Phys Med Rehabil.* 2001;80(1):4-12.

    doi: 10.1097/00002060-200101000-00003

18. Lv H, Wang Z, Tong E, *et al*. Resting-state functional MRI: everything that nonexperts have always wanted to know. *Am J Neuroradiol.* 2018;39(8):1390-1399.

doi: 10.3174/ajnr.A5527

19. Wang X, Wang H, Xiong X, *et al*. Motor imagery training after stroke increases slow-5 oscillations and functional connectivity in the ipsilesional inferior parietal lobule. *Neurorehabilit Neural Repair.* 2020;34(4):321-332.

doi: 10.1177/1545968319899919

20. de Jesus Faria AST. Additive manufacturing of custom-fit orthoses for the upper limb. Master's Thesis. Porto, Portugal: Universidade do Porto; 2017.

21. Meier TB, Nycz CJ, Daudelin A, Fischer GS. The PneuHOPE Hand Exoskeleton: A Platform for Studying Brain Activation During Robot-Facilitated Hand Movement Using fMRI. *IEEE Trans Med Robot Bionics.* 2025;7(1):85-93.

doi: 10.1109/TMRB.2024.3503998

22. Tombari D, Loubinoux I, Pariente J, *et al*. A longitudinal fMRI study: in recovering and then in clinically stable sub-cortical stroke patients. *Neuroimage.* 2004;23(3):827-839.

doi: 10.1016/j.neuroimage.2004.07.058

23. Ward NS, Brown MM, Thompson AJ, Frackowiak RSJ. Neural correlates of motor recovery after stroke: a longitudinal fMRI study. *Brain.* 2003;126(11):2476-2496.

doi: 10.1093/brain/awg245

24. Cramer SC. Treatments to promote neural repair after stroke. *J Stroke.* 2018;20(1):57-70.

doi: 10.5853/jos.2017.02796

25. Dobkin BH, Carmichael ST. The specific requirements of neural repair trials for stroke. *Neurorehabilit Neural Repair* 2016;30(5):470-478.

doi: 10.1177/1545968315604400

26. Buma FE, Raemaekers M, Kwakkel G, Ramsey NF. Brain Function and Upper Limb Outcome in Stroke: A Cross-Sectional fMRI Study. Cappello F, ed. *PLoS ONE.* 2015;10(10):e0139746.

doi: 10.1371/journal.pone.0139746

27. Kitago T, Liang J, Huang VS, *et al*. Improvement after constraint-induced movement therapy: recovery of normal motor control or task-specific compensation? *Neurorehabilit Neural Repair*. 2013;27(2):99-109.

doi: 10.1177/1545968312452631

28. Manganotti P, Acler M, Formaggio E, *et al*. Changes in cerebral activity after decreased upper-limb hypertonus: an EMG-fMRI study. *Magn Reson Imaging.* 2010;28(5):646-652.

doi: 10.1016/j.mri.2009.12.023

29. Schuster-Amft C, Henneke A, Hartog-Keisker B, *et al*. Intensive virtual reality-based training for upper limb motor function in chronic stroke: a feasibility study using a single case experimental design and fMRI. *Disabil Rehabil Assist Technol.* 2015;10(5):385-392.

doi: 10.3109/17483107.2014.908963

30. Crofts A, Kelly ME, Gibson CL. Imaging functional recovery following ischemic stroke: clinical and preclinical fMRI studies. *J Neuroimaging.* 2020;30(1):5-14.

doi: 10.1111/jon.12668